Electronic Supplementary Material (ESI) for Materials Horizons.

Supplemental Materials for

Coalescence-induced transition between unidirectional and bidirectional propagation of droplets

Jiaqian Li[1,2] and Liqiu Wang[1,2*]

[1]*Department of Mechanical Engineering, the University of Hong Kong, Hong Kong*

[2]*HKU-Zhejiang Institute of Research and Innovation (HKU-ZIRI), Hangzhou, Zhejiang 311300, China*

*Correspondence and requests for materials should be addressed to L.W. (lqwang@hku.hk)

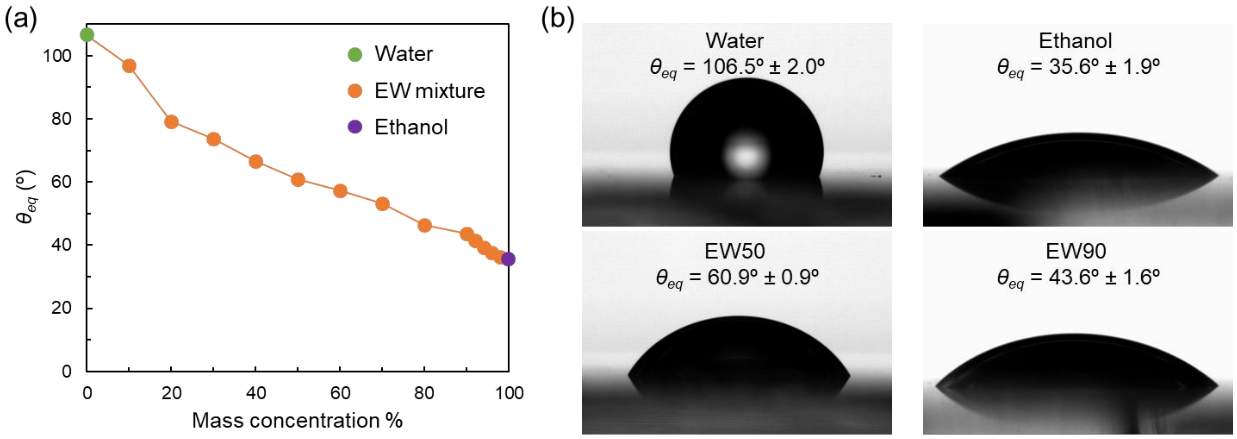

Fig. S1. Wettability characterization on the flat PDMS surface. (**a**) The variation of intrinsic contact angle θ_{eq} under different ethanol mass concentrations. (**b**) Snapshots showing the intrinsic contact angles for water, ethanol, EW50 and EW90 on the flat PDMS surface.

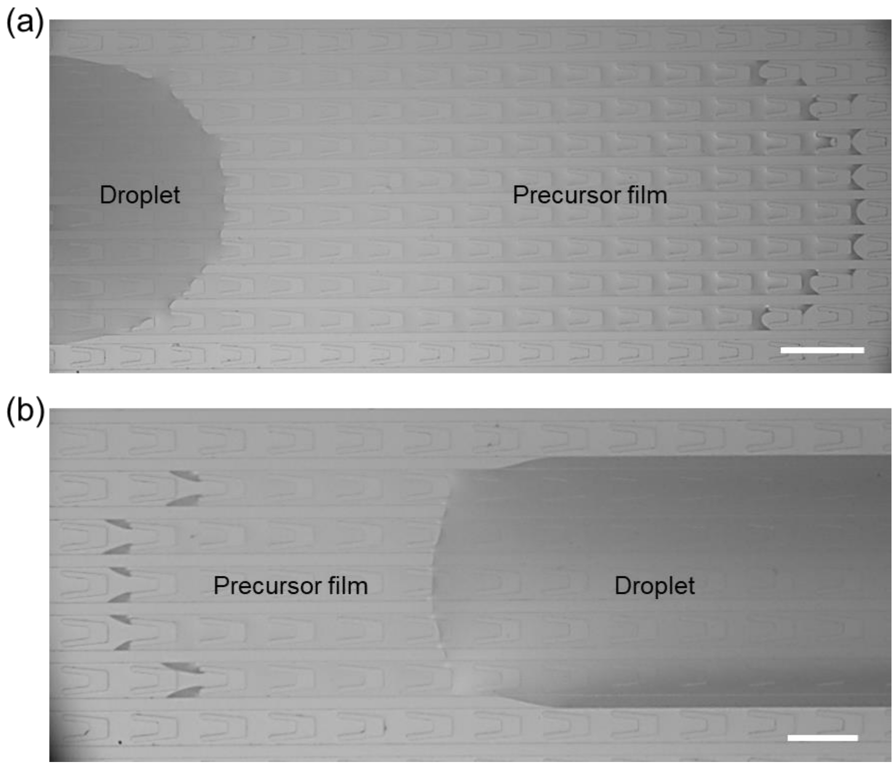

Fig. S2. Precursor film in two directions. (**a**) Snapshot showing that the precursor film is formed preceded by the primary ethanol droplet in the spread direction. (**b**) Snapshot showing that the precursor film is formed ahead of the ethanol droplet in the pin direction. Scale bars: (a) 500 μm; (b) 300 μm.

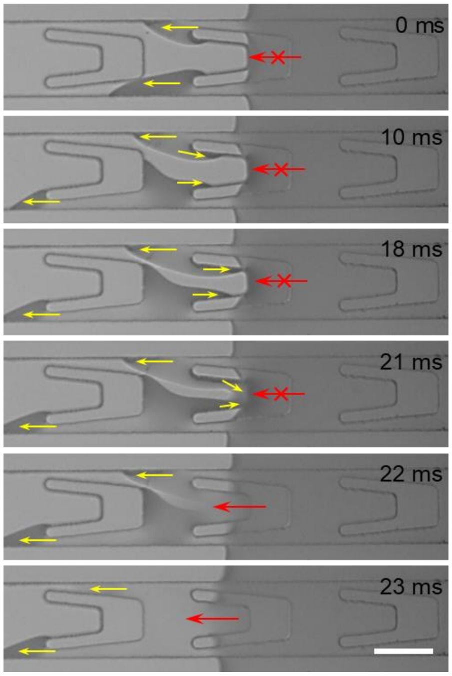

Fig. S3. Mechanism of partially filling cavity during the bidirectional propagation of the ethanol droplet. Since one filament in the side channel advances significantly faster than another one, they cannot integrate together to wet the space between two posts. As a result, two long filaments propagate along the inner corner of the cavity and then a filament ring is formed in the cavity (0 to 21 ms). Subsequently, the droplet edge in the pin direction coalesces with the filament ring and penetrates into the cavity (21 to 23 ms). Red arrows, red arrows with crosses, and yellow arrows represent the propagation of the droplet edge, the pinning of the droplet edge, and the propagation of the precursor liquid, respectively. The scale bar is 100 μm.

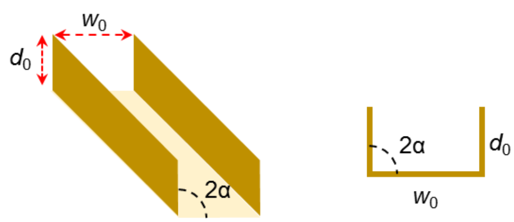

Fig. S4. Schematics of the rectangular channel. w_0 and d_0 are the width and depth of the parallel channel with rectangular cross-section, respectively. α represents the half-angle of the corner between the channel wall and bottom surface.

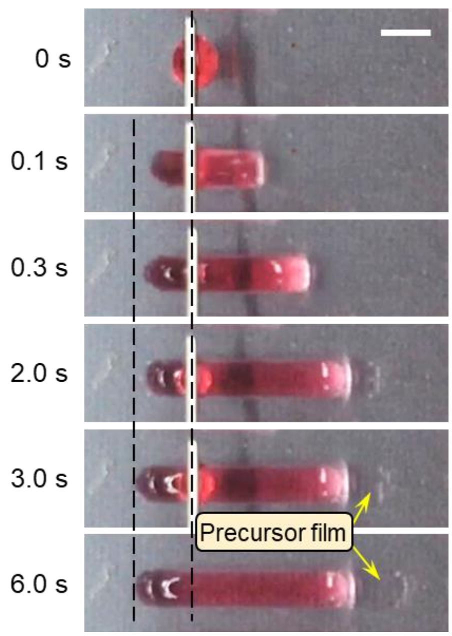

Fig. S5. Nearly bidirectional propagation of the EW90 droplet on the heterogenous surface. Obviously, there is a layer of precursor film ahead of the droplet in two directions. The arrested edge of the EW90 droplet gradually spreads in the pin direction, which is much slower than that in the spread direction. This kind of spreading state is defined as nearly bidirectional droplet spreading. The scale bar is 2 mm.

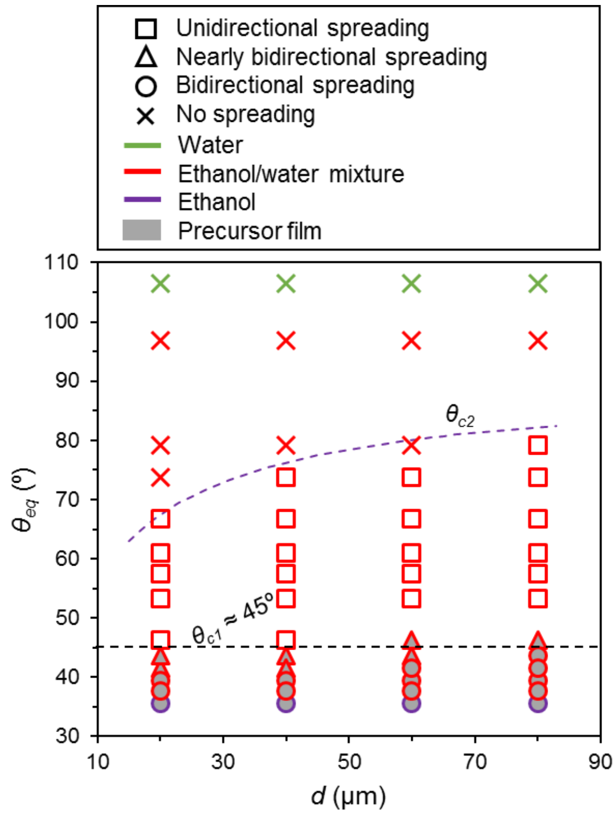

Fig. S6. Effect of the cavity depth on the droplet propagation behaviors and their transitions. The critical angle θ_{c2} is affected by the depth of the channels. The purple dashed line indicates the theoretical result of equation 2. The crosses, squares, circles and triangles represent experimental results of no, unidirectional, bidirectional, nearly bidirectional liquid spreading, respectively. The colors of these symbols denote the different liquids used in the experiments. The gray color filled in the symbols indicates that there is a layer of precursor film advancing ahead of the droplet in the experiments.

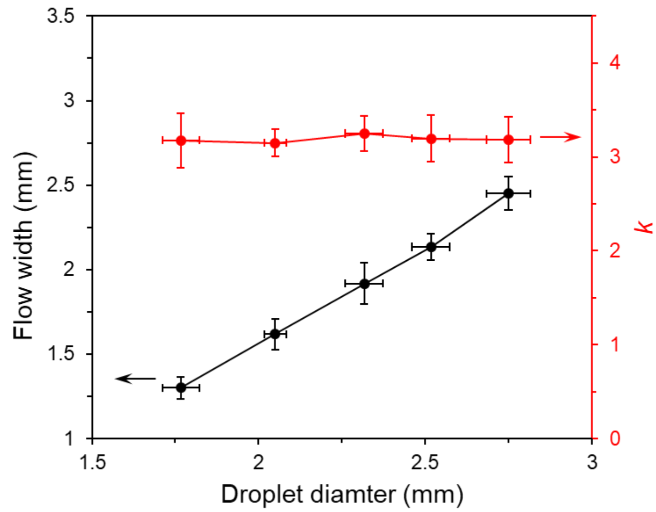

Fig. S7. Effect of the droplet size on the directional flow. The droplet size controls the width of the directional flow, whereas has little effect on the directionality of the flow, in which *k* remains essentially constant. With the increase of the droplet diameter, the directional flow becomes wider. The used liquid here is EW80, and the heterogeneous surface has $\delta \approx 0.32$ and $d \approx 40\mu m$.

Supplementary Movies

Movie S1. Unidirectional propagation of an EW80 droplet on the heterogeneous surface. An EW80 droplet with $\theta_{eq} \approx 46.3^{o}$ preferentially propagates toward the direction of entering the cavity structure, defined as spread direction, and keeps stably pinned in the opposite or pin direction.

Movie S2. Bidirectional propagation of an ethanol droplet on the heterogeneous surface. An ethanol droplet with $\theta_{eq} \approx 35.6^{o}$ prefers to propagate symmetrically along the parallel channels on the heterogenous surface.

Movie S3. Strong pinning of the EW80 droplet on the heterogeneous surface. The edge of the EW80 droplet is stably arrested by the cavity edges after a slight advance in the reverse direction. The cavities remain dry because the short precursor liquid just progresses into the side channels.

Movie S4. Spreading dynamics of the EW80 droplet on the heterogeneous surface. The edge of the EW80 droplet in the spread direction is prone to penetrate into the cavities without the impediment of the cavity edges. As a result, the cavity provides an additional pathway for the spreading of the droplet compared to that in the pin direction.

Movie S5. Pinning breakdown of the ethanol droplet on the heterogeneous surface. The precursor liquid of the ethanol advances ahead of the droplet and penetrates into the cavity structure. Once the cavity is completely filled, the ethanol droplet edge coalesces with the precursor film in the cavity, resulting in the breakdown of strong pinning in the pin direction.

Movie S6. Spreading dynamics of the ethanol droplet on the heterogeneous surface. There is a layer of precursor liquid spreading ahead of the ethanol droplet and filling the cavity in advance. The latter droplet edge subsequently coalesces with the precursor film and progresses forward in the spread direction.